
Visual Haystacks: Answering Harder Questions About Sets of Images

Tsung-Han Wu Giscard Biamby Jerome Quenum Ritwik Gupta
Joseph E. Gonzalez Trevor Darrell David M. Chan

University of California, Berkeley

Abstract

Recent advancements in Large Multimodal Models (LMMs) have made significant progress in the field of single-image visual question answering. However, these models face substantial challenges when tasked with queries that span extensive collections of images, similar to real-world scenarios like searching through large photo albums, finding specific information across the internet, or monitoring environmental changes through satellite imagery. This paper explores the task of Multi-Image Visual Question Answering (MIQA): given a large set of images and a natural language query, the task is to generate a relevant and grounded response. We propose a new public benchmark, dubbed "Visual Haystacks (VHs)," specifically designed to evaluate LMMs' capabilities in visual *retrieval* and *reasoning* over sets of unrelated images, where we perform comprehensive evaluations demonstrating that even robust closed-source models struggle significantly. Towards addressing these shortcomings, we introduce MIRAGE (Multi-Image Retrieval Augmented Generation), a novel retrieval/QA framework tailored for LMMs that confronts the challenges of MIQA with marked efficiency and accuracy improvements over baseline methods. Our evaluation shows that MIRAGE surpasses closed-source GPT-4o models by up to 11% on the VHs benchmark and offers up to 3.4x improvements in efficiency over text-focused multi-stage approaches.

1 Introduction

The development of high-quality visual question-answering (VQA) technologies based on large foundation models marks a significant milestone in bridging the gap between humans and machines, enabling the extraction of insightful information from visual content through natural language questions. However, the scope of existing VQA approaches has predominantly been restricted to single-image analysis, narrowing its utility for addressing more intricate inquiries that involve extensive collections of visual data. Take, for example, the challenges of discerning patterns in vast arrays of medical images, monitoring deforestation through satellite imagery, mapping urban changes using autonomous navigation data, analyzing thematic elements across large art collections, or understanding consumer behavior from retail surveillance footage. Each of these scenarios entails not only visual processing across hundreds or thousands of images but also necessitates cross-image processing of these findings — a task that exceeds the reach of traditional VQA systems.

Addressing this gap necessitates the development of robust Multi-Image Visual Question Answering (MIQA) systems capable of efficiently processing and analyzing extensive collections of images. The core challenges in MIQA lie in the ability to (1) accurately **retrieve** relevant images from a vast pool of potentially unrelated images and (2) **integrate** relevant visual information from these images to correctly answer the question. While recent models capable of MIQA such as Gemini 1.5-pro and GPT-4V are capable of taking multiple images as input (MII-capable) and have overcome key technical hurdles to MIQA (such as long-context learning), it remains unknown if they can perform the retrieval and integration tasks, particularly as the volume and variability of images increases.

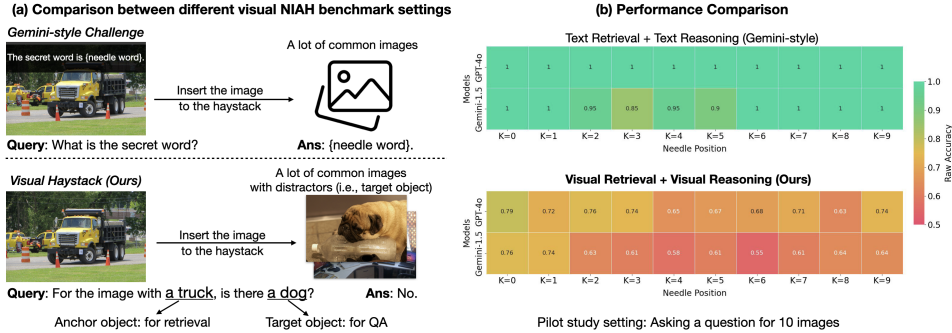


Figure 1: (a) Unlike existing visual Needle-In-A-Haystack (NIAH) challenges [37] that overlay needle information as text directly onto the image, our "Visual Haystacks" (VHs) benchmark is visually focused, requiring the model to retrieve the needle image from the haystack and then reason to answer the specific question using visual contents. (b) We benchmark existing LMMs under different NIAH settings where only one needle image is present among ten images. While traditional visual NIAH challenges overemphasize text retrieval, which can be easily hacked by state-of-the-art models with strong OCR capabilities, they are unable to solve the simple visual questions in VHs.

In this work, we begin by rigorously evaluating the readiness of existing MII capable models for the MIQA task by introducing a new benchmark for MIQA dubbed "Visual Haystacks (VHs)," designed to explicitly test a model's ability to first *retrieve* relevant images and then *integrate* information across those images. While based on existing needle-in-a-haystack (NIAH) evaluations [17, 37], VHs goes beyond simple text/OCR-based needles (For example, Gemini 1.5 Pro is evaluated using text-overlays on images), and leverages needles which require visual reasoning capability ("For the image containing a *cat*, is there a *dog*?"") in both the retrieval and integration stages. Evaluating both open and closed-source models on VHs demonstrates a surprising result: existing MII-capable models fail to answer simple MIQA problems, leading to performance degradation of up to 50% over non-retrieval QA problems. We also notice a dramatic positional-bias phenomenon across these models similar to that noticed in natural-language tasks by Liu *et al.* [29]: when the relevant image is placed deeper within the context, performance degrades even further.

To address these issues, we introduce a simple single-stage training paradigm, "MIRAGE" (Multi-Image Retrieval Augmented Generation), which extends the LLaVA [27] model to handle MIQA tasks. Our proposed paradigm consists of several components, each designed to alleviate key issues in the MIQA task, among them (1) augmenting the image-encoder with a compressive image encoding and (2) leveraging a retrieval-based, query-aware, relevance filter, both aimed at allowing more images given the same context budget, and (3) augmenting the training process with additional targeted synthetic and real MIQA data. Through results on VHs and existing benchmarks for MIQA including RetVQA [19], we demonstrate that our proposed approach outperforms standard retrieval-augmented methods on MIQA benchmarks, is robust to depth in visual-haystack questions, and is more efficient than text-focused multi-stage planning approaches.

To summarize, our contributions are as follows:

- We introduce a new benchmark, "Visual Haystacks (VHs)" which explicitly tests MIQA models on their ability to *retrieve* and *integrate* visual information.
- We conduct comprehensive evaluations of existing open and closed-source models on the VHs benchmark, and demonstrate that not only are existing models incapable of solving the VHs task, but demonstrate notable positional bias for MIQA tasks (similar to the "lost-in-the-middle" phenomena).
- We introduce MIRAGE (Multi-Image Retrieval Augmented Generation), a novel retrieval-aware training framework designed explicitly for MIQA, and demonstrate that it can perform GPT-4o by up to 11% (N=3, Single Needle) on VHs, while remaining up to 3.4x times more efficient than text-focused multi-stage planning approaches.

2 The Visual Haystacks Benchmark (VHs)

The "Needle-In-A-Haystack" (NIAH) challenge [17, 37] has recently become one of the most popular methods for evaluating LLM/LMM systems' ability to process long-context inputs. In this task, essential

information (“the needle”), which contains the answer to a specific question, is embedded within a vast amount of data (“the haystack”). The system must then retrieve the relevant information and answer the question correctly. Building on the NIAH concept, we explore its application in the Multimodal Image Question Answering (MIQA) task. Formally, the MIQA task requires a model to answer a single question (“Q”) given a large number of images ($I = I_0, I_1, I_2, \dots, I_N$). In this scenario, at least one target image contains the answer, while the rest serve as distractors. Evaluating models on this task necessitates a robust benchmark that can accurately measure their performance in retrieving the correct information to do question answering with extensive visual inputs. In this section, we first elaborate on the limitations of existing benchmarks and introduce a new benchmark, dubbed "Visual Haystacks" (VHs). Then, we conduct a comprehensive analysis of existing methods, including open-source, closed-source and long-context LMM solutions, on this benchmark dataset and highlight their limitations.

2.1 Benchmark Construction

Currently, no existing NIAH dataset is designed for reasoning across a large number of images (instead of a text counterpart). The closest example is the demo in the Gemini-v1.5 technical report [37], which created “needle” frames in a long video by overlaying text reading “The secret is Needle” on a frame within the video, and asking the model to retrieve the secret text. While such an approach can evaluate a model’s ability to retrieve content from a large context, this needle image creation approach is overly OCR-centric, essentially allowing the model to perform text retrieval followed by text reasoning, which de-emphasizes the image retrieval and image reasoning components. Furthermore, the challenge included only a single test case, rather than multiple test cases across diverse scenarios, making the evaluation less convincing.

To address these shortcomings, we introduce a new benchmark which we call "Visual Haystacks (VHs)." The VHs dataset (which we release under a CC-BY-4.0 license) is constructed using the COCO dataset (CC-BY-4.0 license) [24], which already has accurate object-level annotations. To generate a question/answer pair, we begin by selecting two objects from COCO’s label set for the question. We then generate the text of the question in one of two settings: a single-needle setting, for which the question is framed as “For the image with anchor object, is there target object?” and a multi-needle setting where the question is framed as either “For all images with anchor object, do all of them contain target object?” or “For all images with anchor object, do any of them contain target object?”. The answers are binary—Yes or No—and are carefully curated to ensure that guessing or relying on common sense reasoning without viewing the image results in a 50% accuracy rate. This design ensures that the anchor object serves as the key for image retrieval, while the target object forms the basis of the actual question during image reasoning.

After selecting the object pairs and determining the answers, we compile the corresponding image haystacks by first extracting the needle images (images containing both the anchor objects). The needle images contain the "anchor object" and may or may not contain the target object based on the answer. Then, these images are paired with multiple negative distractors to form varied haystack sizes, ranging from 1 to 10,000 haystack images. The distractor images are carefully selected to not contain any anchor object (following COCO’s object annotations), however, *some of them contain the target objects* so as to create meaningful distractors. The single-needle mode contains only one needle image in the haystack, while the multi-needle mode includes between two and five needle images. We carefully filter out all images present in the LLaVA instruction fine-tuning set. VHs consists of 880 and 1000 question-answer pairs for single- and multi-needle setting, with an explicit small subset VH_{small} consisting of 100 questions, which can be used for economical evaluation of expensive closed-source models.

As shown in Figure 1 (a), VH is closer to real-world scenarios compared with the prior Gemini-style challenges. It requires models to assess the relevance of each "visual context" to the prompted question and utilize visual reasoning to formulate precise answers. Figure 1 (b) presents an experiment over Gemini-style dataset and ours. The results demonstrate that shifting the benchmark from text-oriented to visual-oriented significantly increases the difficulty for existing MII-capable methods, such as GPT-4 and Gemini, highlighting the importance of our dataset.

2.2 Single-Needle Challenge

In our initial experiments on the VHs dataset, we evaluate several state-of-the-art MII-capable methods (including both open-source and proprietary models including LLaVA-v1.5 [26], GPT-4o [32], Claude-3 Opus, and Gemini-v1.5 [42]). We further include a “Captioning” baseline, a two-stage approach where the images

Method	Tokens/Img	N=1 (Oracle)	N=3	N=5	N=10	N=50	N=100	N=1K	N=10K
Naive									
Question Only (LLama3)	-	0.52	-	-	-	-	-	-	-
Caption-Based (LLaVA + LLama3)	576	0.79	0.67	0.69	0.68	0.59	E	E	E
LMM									
LLaVA-v1.5-7B	576	0.87	0.70	E	E	E	E	E	E
Claude-3 Opus	≈64	0.67	0.54	0.51	0.47	E	E	E	E
Gemini-1.5	≈258	0.87	0.73	0.68	0.64	0.58	0.59	E	E
GPT-4o (low-res)	≈85	0.82	0.68	0.68	0.64	0.57	0.53	E	E
RAG-based									
MIRAGE (Ours)	32	0.81	0.76	0.71	0.66	0.60	0.55	0.49	0.43

Table 1: Results for several models on VHs for single-needle questions. All models experience significant falloff as the size of the haystack (N) increases, indicating that existing approaches are not robust to complex visual-linguistic processing over long visual contexts. E: Exceeds context length.

Method	Oracle	N=5	N=10	N=50	N=100	N=1K	N=10K
Naive							
Question Only (LLama3)	0.48	-	-	-	-	-	-
Caption-Based (LLaVA + LLama3)	0.70	0.70	0.66	0.56	E	E	E
LMM							
Claude-3 Opus	0.55	0.49	0.48	E	E	E	E
Gemini-1.5	0.56	0.51	0.54	0.50	0.52	E	E
GPT-4o (low-res)	0.71	0.65	0.63	0.49	0.52	E	E
RAG-based							
MIRAGE (Ours)	0.57	0.56	0.54	0.51	0.50	0.48	0.49

Table 2: Performance on VHs for multi-needle questions. We can see that all visually-aware models perform poorly, indicating that models find it challenging to implicitly integrate visual information. E: Exceeds context length.

are first captioned using LLaVA, and then the question is answered using the text content of the resulting captions. For each setting, we leveraged the VHS_{small} dataset, and reported the bootstrapping average results using 75 of the 100 samples for each bootstrap sample, resulting in standard deviations between 3-4% for all experiments. The results presented in Table 1 reveal several critical insights. Overall, we notice that even though the models perform well on existing NIAH datasets (Figure 1), performance is significantly worse on the VHs dataset across the board. Because oracle results remain high, it is likely that existing approaches **primarily struggle with visual retrieval**, particularly in the presence of challenging detractor samples.

Interestingly, chaining a captioning model (LLaVA [27]) with an LLM aggregator (LLama-3 [1]) is straightforward and effective, suggesting that the issues on the task are largely limited to visual processing capabilities and not information processing behavior. Unfortunately, this approach is generally inadequate for the MIQA challenge due to its computational expense and limited context lengths. For instance, when processing 100 images, it takes over 3 minutes to answer a single question (see Figure 4 for full runtime results), and 100 captions exceed the 8K context length of LLama3, leading to inaccurate and nonsensical outputs.

Beyond the performance of the text-only baselines, it is important to look at the divide between open-source and closed-source LMMs. Unfortunately, open-source LMMs such as LLaVA suffer primarily from context-length issues, taking at most three images in their shorter trained context lengths. Proprietary long-context models can handle up to one hundred images, but despite their technical capability of handling such long contexts, these models are highly susceptible to distractions from irrelevant images. Further, even though these models are long-context, they are not capable of handling very large haystacks. For 1K and larger haystacks, Gemini-v1.5 and GPT-4o with the low-resolution encoding scheme reject most API requests as it exceeds the payload size limits.

In addition to being prone to distractions, we also found the accuracy of LMMs is very sensitive to the position of the needle image within the input sequence, as shown in Figure 2. LLaVA performs better when the needle image is placed immediately before the question (suffering up to a 26.5% degradation when this is not the case), while proprietary models perform better when the image is at the beginning (leading to up to a 28.5% performance degradation). This pattern suggests a challenge similar to the "loss-in-the-middle" phenomenon in NLP [29], where relevant information is contained in either the beginning or end of the context, leading to inherent positional biases in the performance of the model. Interestingly, this pathology was not observed in the prior Gemini-style NIAH challenge, which required only text retrieval and reasoning, as shown in the top row in Figure 1 (b). This interesting result clearly highlights the importance of vision-specific NIAH benchmarks such as VHs.

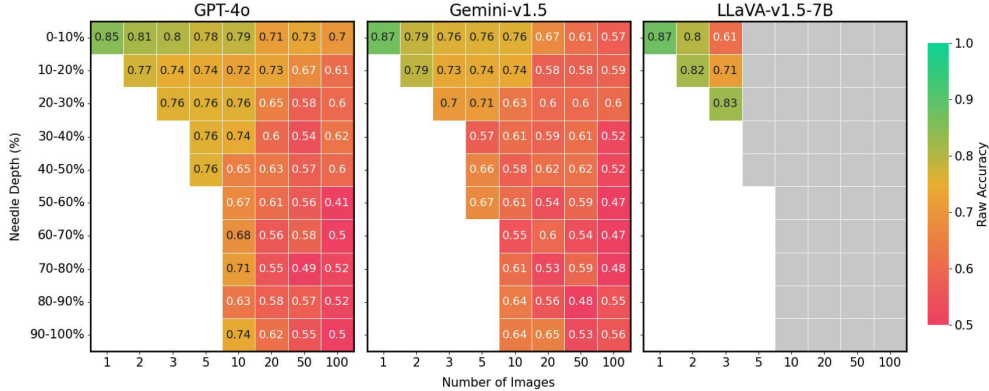


Figure 2: Plots showing needle position, vs. performance on the VHS benchmark for several image settings. We can see that for existing LMMs, the needle position is extremely important, with performance degradation of up to 41% when the needle is not placed in the optimal location in the input context. The gray boxes in the LLaVA results indicate that these experiments exceed the available context length (and performance is accordingly random).

2.3 Multi-Needle Challenge

We use a similar setup to [subsection 2.2](#) to evaluate in the multi-needle setting. The results of the multi-needle challenge are shown in [Table 2](#). Overall, we see similar (yet more dramatic) results to the single-needle setup. Here, however, the captioning approach has the best performance, suggesting that using an external LLM to integrate multiple text inputs is superior to an LMM’s internal capability to aggregate information from multiple image inputs. Similar to the single-needle case, however, the captioning baseline suffers from the same computational burden and performs poorly when $N=100$ due to context length limitations. It is notable that LMMs alone perform quite poorly on this task, specifically, Gemini-1.5 and Claude-3’s performance on multi-image reasoning was very poor, almost guessing the answer most of the time, indicating its inability to aggregate information from multiple images effectively.

3 MIRAGE: Multi-Image Retrieval Augmented Generation

To develop an open-source framework for MIQA capable of improved performance on the VHS benchmark, we introduce MIRAGE, a new framework for training an open-source MII-capable model. This framework addresses several critical challenges for baseline performance in MIQA including: (1) reducing the required tokens per image to allow the input of more images, (2) incorporating a lightweight retriever module trained inline with the LMM to filter out irrelevant images, and (3) providing an open-source training dataset and recipe designed for multi-image reasoning that is robust against noisy images and the position of the correct image. We elaborate on these components in the subsequent sections.

3.1 Model Architecture

As shown in [Figure 3](#), MIRAGE is a RAG-based solution extended from LLaVA-v1.5-7B [26], where the input prompt to the model is structured as "Image 1: <img_token>, Image 2: <img_token>, ... <Actual Question>". First, similar to LLaVA, each image is passed through a frozen CLIP image encoder to extract patch-level features (576 tokens). To reduce the token-intensity, we first apply an image compressor, designed to reduce the overall token intensity by reducing the number of tokens per image. In this work, we leverage a Q-former [21], a light-weight transformer model with $K = 32$ learned query vectors cross-attending to the full 576 patch features, to compress the patch-level features from 576 to 32 tokens/image (a 18x reduction in token intensity). After this initial reduction, following LLaVA, the output passes through two MLP layers with GELU activation functions [13] which helps adapt to the LLM’s input dimension. We explore this choice compared to other compressors further in [Table 4](#).

While the token reduction via the Q-former alone allows MIRAGE to handle more than 50 images as input with minimal reduction in accuracy (see [Table 3](#)), in MIQA we often want to answer questions over many hundreds or thousands of images. Such limitations lend themselves to retrieval-based approaches, in which a small amount of additional processing is performed per-image to determine if the image is relevant, and the LMM (which is context-length aware) is run against the reduced relevant set. In order to

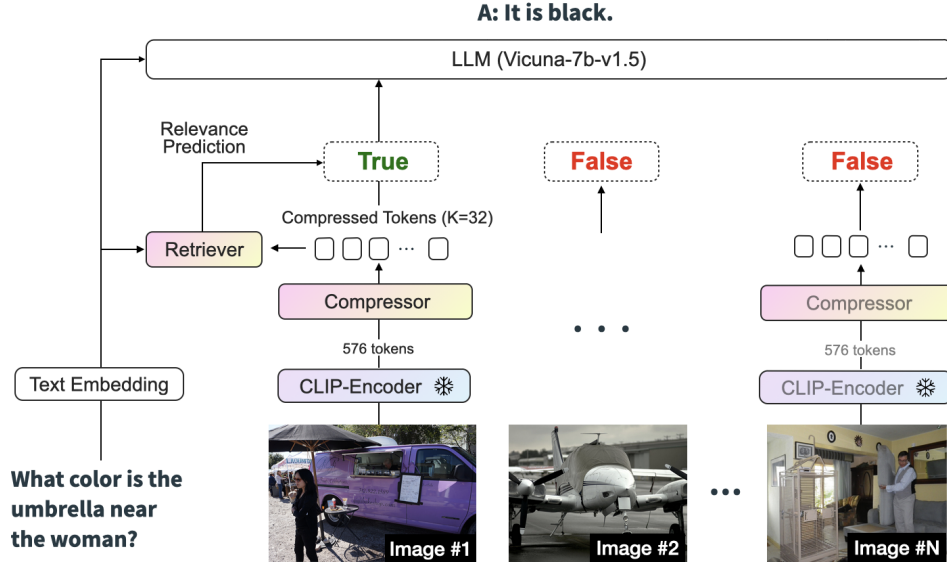


Figure 3: Model Overview: MIRAGE handles questions and images through several steps: encoding features with CLIP, compressing image features with our Q-Former, calculating relevance scores with a retriever, and feeding only relevant images to the LLM. During instruction finetuning, the model is supervised for the next token prediction and the relevance prediction task, utilizing Binary Cross Entropy loss between the ground truth 0, 1 and the predicted number.

enable this capability, we augment our filter with a hard-pass filter or “retriever.” While this hard-pass filter can take many forms (such as a CLIP-similarity threshold), we found it effective to train a query-aware retrieval model in-line with the next-token prediction task. Formally, given a set of images, I made up of image tokens $\{i_0, \dots, i_n\}$, it is our goal to retain the minimal subset $I_{\min} \subset I$ such that we can still accurately answer the query Q . Let the image encoding module as a function $\psi(I)$, we can get:

$$F_i, R_i = \psi(I_i, Q), \quad (1)$$

where F_i represents image features and R_i represents the relevance score of the image of Image I . In practice, our retriever module consists of a single-layer MLP on top of the temporally pooled query and image features, along with a sigmoid activation to predict a 0/1 value. Such an approach has significant benefits, as the retriever is query-aware, and can make use of the information from the query to determine image relevance. A downside to this approach, however, is that we can no longer use efficient data structures (such as LSH) for k-nearest neighbors recall (unlike a split-head/metric-based model such as CLIP [35]). It remains interesting and exciting future work to explore if high-recall query-aware split-head models can be created. The output of the retriever module is a score between 0 and 1 indicating the relevance of the image to the query. During training, this output is optimized against the ground truth relevance, while during inference, only images deemed relevant (in our experiments, having relevance score > 0.5 are forwarded to the LMM). We explore this choice further in [section 4](#).

After applying the image token reduction and retrieval filtering, the LLM takes the resulting set of visual features and the encoded questions as input. Similar to existing LMMs, we concatenate the image and query inputs and fine-tune the model from an existing LLM using next-token prediction.

3.2 Model Training

Training Data: While single-image QA data is relatively plentiful, open-source data for MIQA is quite limited in the community. Thus, the training data for MIRAGE contains data from two key sources: (1) Existing MIQA data, and (2) Synthetic MIQA data derived from single-image QA datasets. We first included all publicly available MIQA training sets, including RetVQA [34], SlideVQA [41], and WebQA [7]. RETVQA has the largest available dataset, with about 377K questions curated from Visual Genome data. However, these multi-image questions come from scene graphs and cover a very limited domain, such as counting, relationships, and object attributes. WebQA contains diverse images and questions from Wikipedia, and SlideVQA

Method	MIQA (RetVQA)			Single-Image QA							
	Recall	Precision	VQA Acc.	VQAv2	GQA	Vizwiz	TextVQA	POPE	MMB	MMB-CN	MM-Vet
Qwen-VL-Chat [2]	-	-	0.0*	78.2	57.5	38.9	61.5	-	60.6	56.7	-
LLaVA-v1.5-7B [26]	-	-	30.6	78.5	62.0	50.0	58.2	85.9	64.3	58.3	31.1
GPT-4o [32]	-	-	34.6	-	-	-	-	-	-	-	-
GPT-4 [33]	-	-	-	77.2	-	-	78.0	-	-	-	-
Gemini-v1.5 [42]	-	-	32.2	73.2	-	-	73.5	-	-	-	-
LWM [28]	-	-	-	55.8	44.8	11.6	18.8	75.2	-	-	9.6
MI-BART [34]	-	-	76.5	-	-	-	-	-	-	-	-
MIRAGE (Ours)	80.5	49.9	70.8	70.0	55.2	40.1	46.3	83.4	57.6	48.8	25.8

Table 3: Comparative performance of methods on multi-image and single-image QA tasks. We can see that MIRAGE has strong recall/precision capabilities, strong multi-image QA performance, and competitive single-image QA performance. *Qwen-VL-Chat is also over-fit to the VG dataset, and produces object bounding boxes instead of answers for the RetVQA queries.

Method	Tokens/Img	VQAv2	GQA	Vizwiz	TextVQA	POPE	MMB	MMB-CN	MM-Vet
Original LLaVA	576	78.5	62.0	50.0	58.2	85.9	64.3	58.3	31.1
3x3 Max-Pooling	64	68.7	56.2	41.3	48.5	83.0	59.2	49.3	24.3
Global Avg. Pooling	1	62.5	51.3	37.7	45.5	79.6	55.0	45.5	18.9
MIRAGE/Q-Former (Ours)	32	72.8	56.6	48.0	47.1	83.9	61.5	55.0	27.3

Table 4: Exploration of various token reduction methods. We can see that the Q-former is most efficient at reducing the number of tokens while retaining most of the general QA performance.

includes complex questions for multiple slides, but these datasets only include 19K and 12K questions, respectively. In these three datasets, there are only one or two relevant images, in a set of 15-30 total images.

Second, to augment our training data and enhance diversity, we adapted the LLaVA single-image training data to a multi-image format. While a straightforward method for synthetic data augmentation would be to find many distractor images for a single-image QA, identifying suitable distractors is challenging, and many questions naturally apply to multiple images, complicating dataset construction. To avoid such situations, we filter questions for similar content (based on keyword frequency, retaining unique questions), and then randomly sample two to ten distractor images from unrelated subsets. This process results in an instruction-tuning dataset containing 1.2M samples. We further shuffle the images within each instruction-tuning pair during training to ensure the relevant images can appear in any position, aiming to make our model insensitive to the needle image’s position.

Training Procedure: Similar to LLaVA, MIRAGE follows a two-stage training paradigm: pre-training and fine-tuning. In the pre-training stage, we freeze the CLIP visual encoder and LLM backbone, disable the retriever functions, and only train the Q-Former compressor and the MLP feature alignment layers using the next-token prediction task. We use the Share-GPT captioning data [27] for pretraining. In the fine-tuning stage, we apply the retriever and fine-tune the entire model (except for the fixed CLIP visual encoder) using the training dataset described above. In addition to the conventional next token prediction loss, we also co-train the retriever with binary cross-entropy loss, assigning a weight of 5.0 to positive samples to emphasize recall and address the imbalance due to the many zero cases. We train the model for one epoch on 8 A100 GPUs (taking approximately two days), during which, in the first 75% of training, we always pass only the features of relevant images to the LLM. For the remaining time, we occasionally feed several distractor images to the model, to improve robustness to imperfect retrieval.

4 Results & Discussion

Visual Haystacks: The performance of MIRAGE on the VHs task is shown in Table 1 and Table 2. In the single-needle challenge, our model achieves competitive oracle performance compared to existing approaches, however performance is somewhat lower due to the underlying token compression. Overall, MIRAGE outperforms GPT-4o (low-resolution) across all settings and surpasses Gemini-v1.5-pro and Claude-3 Opus with haystack sizes below 50 images (despite being significantly cheaper on a per-token basis). In the multi-needle setting, MIRAGE outperforms Gemini-v1.5-pro (even in oracle performance), suggesting that MIRAGE is significantly better than Gemini at simple reasoning across multiple images (which makes sense, given the multi-image aware training). Unfortunately, MIRAGE under-performs compared to GPT-

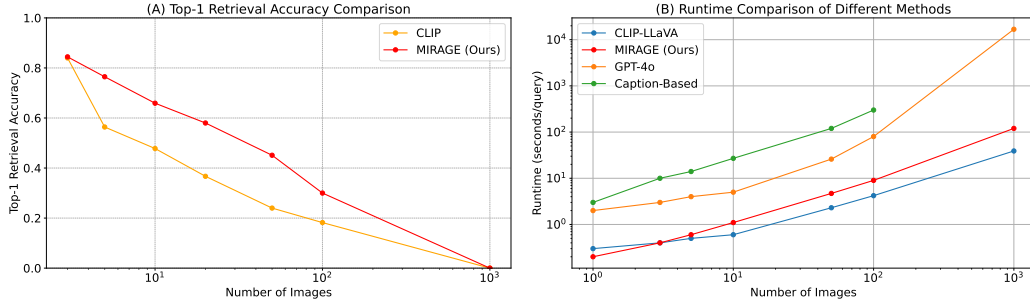


Figure 4: Comparison between MIRAGE retriever and CLIP retriever across both performance and runtime. We can see that while CLIP is slightly faster, MIRAGE has significantly higher recall, which impacts downstream performance. Both MIRAGE approaches with a retrieval component are significantly more efficient than GPT-4o and Caption-based baselines.

4o and caption-based baselines in oracle performance, suggesting that there remains significant room for future work in the reasoning component. We hypothesize that such degraded oracle performance is because existing training sets only require models to learn from at most two images, limiting our model’s ability to handle tasks requiring reasoning across more than three images, an issue that can be resolved with future developments to MIQA datasets. MIRAGE shines, however, in retrieval performance, and enables much longer contexts than GPT-4o and Gemini alone, which cannot handle the 1K and 10K image scenarios.

Conventional VQA Tasks: We also compare MIRAGE with other methods on conventional VQA tasks, including the RetVQA multi-image task [34] and several single-image QA tasks, VQA-v2 [10], GQA [15], VizWiz [11], TextVQA [39], POPE [22], MMB [30], MMB-CN [30], and MM-Vet [51]. In all cases, we follow standard evaluation procedures from either RetVQA [34] or LLaVA [27]. As shown in Table 3, MIRAGE is the only method that is capable of both multi-image QA and single-image QA. Open-source models (LLaVA [27], Qwen-VL-Chat [2]) struggle with the multi-image QA task, likely due to insufficient context length and over-specialized training (e.g., over-fitting in Qwen-VL-Chat or lack of multi-image QA diversity in LLaVA’s dataset). Similarly, commercial long-context LMMs also perform poorly on the multi-image reasoning task, confirming the results demonstrated by VHS in section 2, likely due to similar reasons.

Image Token Compression Scheme: The goal of MIRAGE is to enable future research into MIQA tasks. One of the most important questions in such tasks is how we can reduce the context length required per image. To evaluate this, we compared several different token compression schemes, including token max pooling and average-pooling compression of an image to a single token. In this experiment, all models are trained on LLaVA’s single-image instruction fine-tuning dataset, and the retriever is disabled. The results are shown in Table 4. While previous work claims Q-Former is sub-optimal [9], our results show that Q-Former maintains reasonable performance while reducing context length.

MIRAGE retriever vs. CLIP: While MIRAGE trains the retrieval model inline, it is also possible to use an external retrieval module such as CLIP [35] to perform lookup prior to passing images to the downstream LLM. To explore this question, we compare the single-stage MIRAGE retriever with using CLIP as the retriever on the VHS benchmark in Figure 4. This experiment demonstrates that while CLIP is somewhat faster, it struggles with recall, a critical metric for the MIRAGE system, as poor recall leads to necessary information being dropped before even making it to the LLM for analysis.

4.1 Limitations and Societal Impact

VHS: While VHS is the first benchmark to investigate how LMMs can retrieve and reason across sets of images, it has some notable limitations. The primary limitation of the benchmark is the scope: since it is based on MS-COCO images, it inherits the implicit biases in the dataset including notable gender, race, and location biases [12, 5, 14, 44]. It is important to work in the future toward developing benchmarks that do not favor models that prefer data having such biases. Beyond such implicit biases, COCO objects are also limited to 80 categories - strong performance on the VHS benchmark does not imply that the model will generalize well to all MIQA problems. Finally, the VHS benchmark is primarily template-based, which means that it does not evaluate the language reasoning capabilities of the LLM. A more complex benchmark would require making more detailed inferences, and require multi-hop reasoning across a wider range of open-domain object sets.

MIRAGE: MIRAGE is significantly more efficient than its LLaVA base, while simultaneously performing better on many MIQA benchmarks. To perform well on MIQA benchmarks, however, we note that MIRAGE sacrifices some single-image performance, likely due to inefficiencies in the multi-task training setup. It remains interesting and necessary for future work to explore how such approaches can retain single-image performance while improving multi-image capabilities. It is also important to recognize that as a large multi-modal model, the potential for misuse of the model exists. Many of the impacts of such models are well studied in other related works [4, 27, 26]. Recognizing this, MIRAGE inherits the safety mechanisms from the LLaVA code-base [27], and includes relevant training details in a fully public code release.

5 Related Work

Ours is not the first work to address the MIQA problem. Similar to our work, Bansal *et al.* [3] introduce a method for multi-image question answering, however in their approach, all of the images (up to 10) are relevant to the question, and their method does not contain a retrieval component. Penamakur *et al.* [34] propose a dataset and method for retrieval-based visual question answering (RetVQA), and share with our work the fact that answers must be gleaned from a set of both relevant and irrelevant images. However, their work differs from ours in two key ways: (1) RetVQA question contexts contain at most two relevant images, meaning that models do not have to reason across many images, largely sidestepping the problem of limited context length, and (2) their approach only allows for small image worlds (up to 30), meaning that they can use a pairwise encoder for each image, and they do not need to search over a large dataset of images potentially containing distractors, limiting the efficiency of their approach. Finally, they are only able to perform question answering over the images, whereas we pursue a method that can additionally perform more complex reasoning tasks given the images in the dataset.

Similar to our MIRAGE approach is Chen *et al.* [8] and Yasunaga *et al.* [49] which both retrieve multiple visual documents to answer queries. In the case of Chen *et al.* [8], the queries are open-ended question answering, and thus, are not grounded within a particular set of context images. Yasunaga *et al.* [49] focuses on one and few-shot classification and image generation, and does not use their multi-image retrieval to answer aggregated questions about those images. In single-image QA, image retrieval in large multimodal models (LMMs) has been explored using “retrieval-tokens” [20], however, it is unclear how such an approach would scale to multi-image QA problems with multiple relevant images. In addition to general QA, several other works contain domain-specific multi-image QA problems, including Slide VQA [41], Multimodal QA [40], WebQA [7] and Document VQA [43], however, none are explicitly designed to answer integration questions across multiple images from a subset of large, unrelated images (like VHs).

Outside of VQA, In traditional NLP, retrieving small passages or single documents from large-scale corpuses has proven effective. Zhang *et al.* [52] introduces a method which fine-tunes LLMs on both relevant and irrelevant documents to support better RAG performance, but does not train an explicit query-aware filter or compression module. ATLAS [16] treats documents as latent variables during training, allowing for efficient retrieval, but requires a complex joint-training setup. Similarly, several methods [38, 36, 6, 18] have demonstrated success with zero or few-shot augmentation of standard LLM contexts with retrieved documents. Beyond context augmentation, several traditional NLP approaches [25, 45, 47, 31, 46, 48] have demonstrated that fine-tuning LLMs to be robust to noisy RAG outputs can lead to performance improvements.

MIQA vs. Video-QA: While several methods have been developed for video question answering (such as Video-LLaVA [23]), the task of answering questions over video is fundamentally different from MIQA. While models that can solve MIQA can often solve video tasks, the inverse is not true, as video frames contain many frame-wise inter-dependencies that are exploited by encoder models (such as MAG-ViT [50] which use temporal blocks, or frame-subsampling, which drops closely related frames). MIQA has independent images, rendering most video models inadequate for this task. It is an interesting direction for future work to explore how to connect MIQA and Video-QA, particularly across the data dimension, wherein Video-QA datasets could provide useful training data for MIQA models.

6 Conclusion

In this work, we introduce “Visual Haystacks” (VHs), a new benchmark for multi-image question answering, designed to test a large multi-modal model’s ability to *retrieve* relevant images from a large collection of unrelated inputs, and *reason* about those images. We show that VHs is significantly more informative than existing NIAH benchmarks based on OCR/Text-finding capabilities and that both open and closed-source models

struggle with this task. To help close the performance gap, we further introduce MIRAGE, a training framework designed for open-source models capable of answering both single-image and multi-image questions, and demonstrate that it can outperform Gemini 1.5 in the VHs benchmark in almost all scenarios while being 3x more efficient than multi-stage pipeline methods. Both VHs and MIRAGE represent some of the first concrete steps towards large MII models capable of answering questions over thousands or tens of thousands of unrelated images. While they represent strong steps forward, the problem is far from solved, and we hope that this benchmark and framework will inspire continued research in MII models and the MIQA problem.

Acknowledgements We thank Lisa Dunlap, Boyi Li, and Xudong Wang for their invaluable feedback during the discussions. This project was primarily supported by a grant from the National Geospatial-Intelligence Agency (Grant No. HM0476-22-1-2001). Authors, as part of their affiliation with UC Berkeley, were supported in part by the National Science Foundation, US Department of Defense, and/or the Berkeley Artificial Intelligence Research (BAIR) industrial alliance program, as well as gifts from Anyscale, Astronomer, Google, IBM, Intel, Lacework, Microsoft, Mohamed Bin Zayed University of Artificial Intelligence, Samsung SDS, Uber, and VMware. Any opinions, findings, conclusions or recommendations expressed in this material are those of the author(s) and do not necessarily reflect the views of NGA, DoD, or the US government. The paper is approved for public release in accordance with NGA-U-2024-01397.

References

- [1] Meta AI. Introducing meta llama 3: The most capable openly available llm to date, 2024.
- [2] Jinze Bai, Shuai Bai, Shusheng Yang, Shijie Wang, Sinan Tan, Peng Wang, Junyang Lin, Chang Zhou, and Jingren Zhou. Qwen-vl: A versatile vision-language model for understanding, localization, text reading, and beyond. *arXiv preprint arXiv:2308.12966*, 2023.
- [3] Ankan Bansal, Yuting Zhang, and Rama Chellappa. Visual question answering on image sets. In *Computer Vision—ECCV 2020: 16th European Conference, Glasgow, UK, August 23–28, 2020, Proceedings, Part XXI 16*, pages 51–67. Springer, 2020.
- [4] Emily M Bender, Timnit Gebru, Angelina McMillan-Major, and Shmargaret Shmitchell. On the dangers of stochastic parrots: Can language models be too big? In *Proceedings of the 2021 ACM conference on fairness, accountability, and transparency*, pages 610–623, 2021.
- [5] Shruti Bhargava and David Forsyth. Exposing and correcting the gender bias in image captioning datasets and models. *arXiv preprint arXiv:1912.00578*, 2019.
- [6] Sebastian Borgeaud, Arthur Mensch, Jordan Hoffmann, Trevor Cai, Eliza Rutherford, Katie Millican, George Bm Van Den Driessche, Jean-Baptiste Lespiau, Bogdan Damoc, Aidan Clark, et al. Improving language models by retrieving from trillions of tokens. In *International conference on machine learning*, pages 2206–2240. PMLR, 2022.
- [7] Yingshan Chang, Mridu Narang, Hisami Suzuki, Guihong Cao, Jianfeng Gao, and Yonatan Bisk. Webqa: Multihop and multimodal qa. In *Proceedings of the IEEE/CVF Conference on Computer Vision and Pattern Recognition*, pages 16495–16504, 2022.
- [8] Wenhui Chen, Hexiang Hu, Xi Chen, Pat Verga, and William Cohen. Murag: Multimodal retrieval-augmented generator for open question answering over images and text. In *Proceedings of the 2022 Conference on Empirical Methods in Natural Language Processing*, pages 5558–5570, 2022.
- [9] Xiaoran Fan, Tao Ji, Changhao Jiang, Shuo Li, Senjie Jin, Sirui Song, Junke Wang, Boyang Hong, Lu Chen, Guodong Zheng, et al. Mousi: Poly-visual-expert vision-language models. *arXiv preprint arXiv:2401.17221*, 2024.
- [10] Yash Goyal, Tejas Khot, Douglas Summers-Stay, Dhruv Batra, and Devi Parikh. Making the v in vqa matter: Elevating the role of image understanding in visual question answering, 2017.
- [11] Danna Gurari, Qing Li, Abigale J. Stangl, Anhong Guo, Chi Lin, Kristen Grauman, Jiebo Luo, and Jeffrey P. Bigham. Vizwiz grand challenge: Answering visual questions from blind people, 2018.
- [12] Lisa Anne Hendricks, Kaylee Burns, Kate Saenko, Trevor Darrell, and Anna Rohrbach. Women also snowboard: Overcoming bias in captioning models. In *Proceedings of the European conference on computer vision (ECCV)*, pages 771–787, 2018.
- [13] Dan Hendrycks and Kevin Gimpel. Gaussian error linear units (gelus). *arXiv preprint arXiv:1606.08415*, 2016.
- [14] Yusuke Hirota, Yuta Nakashima, and Noa Garcia. Gender and racial bias in visual question answering datasets. In *Proceedings of the 2022 ACM Conference on Fairness, Accountability, and Transparency*, pages 1280–1292, 2022.
- [15] Drew A. Hudson and Christopher D. Manning. Gqa: A new dataset for real-world visual reasoning and compositional question answering, 2019.

- [16] Gautier Izacard, Patrick Lewis, Maria Lomeli, Lucas Hosseini, Fabio Petroni, Timo Schick, Jane Dwivedi-Yu, Armand Joulin, Sebastian Riedel, and Edouard Grave. Atlas: Few-shot learning with retrieval augmented language models. *Journal of Machine Learning Research*, 24(251):1–43, 2023.
- [17] Gregory Kamradt. Llmtest_needleinahaystack, 2023. GitHub repository.
- [18] Urvashi Khandelwal, Omer Levy, Dan Jurafsky, Luke Zettlemoyer, and Mike Lewis. Generalization through memorization: Nearest neighbor language models. *arXiv preprint arXiv:1911.00172*, 2019.
- [19] Abhinav Khattar, Aviral Joshi, Har Simrat Singh, Pulkit Goel, and Rohit Prakash Barnwal. Analysis on image set visual question answering. *arXiv preprint arXiv:2104.00107*, 2021.
- [20] Jing Yu Koh, Ruslan Salakhutdinov, and Daniel Fried. Grounding language models to images for multimodal inputs and outputs. 2023.
- [21] Junnan Li, Dongxu Li, Silvio Savarese, and Steven Hoi. Blip-2: Bootstrapping language-image pre-training with frozen image encoders and large language models. In *International conference on machine learning*, pages 19730–19742. PMLR, 2023.
- [22] Yifan Li, Yifan Du, Kun Zhou, Jinpeng Wang, Wayne Xin Zhao, and Ji-Rong Wen. Evaluating object hallucination in large vision-language models, 2023.
- [23] Bin Lin, Bin Zhu, Yang Ye, Munan Ning, Peng Jin, and Li Yuan. Video-llava: Learning united visual representation by alignment before projection. *arXiv preprint arXiv:2311.10122*, 2023.
- [24] Tsung-Yi Lin, Michael Maire, Serge Belongie, James Hays, Pietro Perona, Deva Ramanan, Piotr Dollár, and C Lawrence Zitnick. Microsoft coco: Common objects in context. In *Computer Vision—ECCV 2014: 13th European Conference, Zurich, Switzerland, September 6–12, 2014, Proceedings, Part V 13*, pages 740–755. Springer, 2014.
- [25] Xi Victoria Lin, Xilun Chen, Mingda Chen, Weijia Shi, Maria Lomeli, Rich James, Pedro Rodriguez, Jacob Kahn, Gergely Szilvasy, Mike Lewis, et al. Ra-dit: Retrieval-augmented dual instruction tuning. *arXiv preprint arXiv:2310.01352*, 2023.
- [26] Haotian Liu, Chunyuan Li, Yuheng Li, and Yong Jae Lee. Improved baselines with visual instruction tuning, 2023.
- [27] Haotian Liu, Chunyuan Li, Qingyang Wu, and Yong Jae Lee. Visual instruction tuning. In *NeurIPS*, 2023.
- [28] Hao Liu, Wilson Yan, Matei Zaharia, and Pieter Abbeel. World model on million-length video and language with ringattention. *arXiv preprint arXiv:2402.08268*, 2024.
- [29] Nelson F Liu, Kevin Lin, John Hewitt, Ashwin Paranjape, Michele Bevilacqua, Fabio Petroni, and Percy Liang. Lost in the middle: How language models use long contexts. *Transactions of the Association for Computational Linguistics*, 12:157–173, 2024.
- [30] Yuan Liu, Haodong Duan, Yuanhan Zhang, Bo Li, Songyang Zhang, Wangbo Zhao, Yike Yuan, Jiaqi Wang, Conghui He, Ziwei Liu, Kai Chen, and Dahua Lin. Mmbench: Is your multi-modal model an all-around player?, 2024.
- [31] Zihan Liu, Wei Ping, Rajarshi Roy, Peng Xu, Mohammad Shoeybi, and Bryan Catanzaro. Chatqa: Building gpt-4 level conversational qa models. *arXiv preprint arXiv:2401.10225*, 2024.
- [32] OpenAI. Hello gpt-4o, 2024.
- [33] OpenAI, Josh Achiam, Steven Adler, Sandhini Agarwal, Lama Ahmad, Ilge Akkaya, Florencia Leoni Aleman, Diogo Almeida, Janko Altschmidt, Sam Altman, Shyamal Anadkat, Red Avila, Igor Babuschkin, Suchir Balaji, Valerie Balcom, Paul Baltescu, Haiming Bao, Mohammad Bavarian, Jeff Belgum, Irwan Bello, Jake Berdine, Gabriel Bernadett-Shapiro, Christopher Berner, Lenny Bogdonoff, Oleg Boiko, Madelaine Boyd, Anna-Luisa Brakman, Greg Brockman, Tim Brooks, Miles Brundage, Kevin Button, Trevor Cai, Rosie Campbell, Andrew Cann, Brittany Carey, Chelsea Carlson, Rory Carmichael, Brooke Chan, Che Chang, Fotis Chantzis, Derek Chen, Sully Chen, Ruby Chen, Jason Chen, Mark Chen, Ben Chess, Chester Cho, Casey Chu, Hyung Won Chung, Dave Cummings, Jeremiah Currier, Yunxing Dai, Cory Decareaux, Thomas Degry, Noah Deutsch, Damien Deville, Arka Dhar, David Dohan, Steve Dowling, Sheila Dunning, Adrien Ecoffet, Atty Eleti, Tyna Eloundou, David Farhi, Liam Fedus, Niko Felix, Simón Posada Fishman, Juston Forte, Isabella Fulford, Leo Gao, Elie Georges, Christian Gibson, Vik Goel, Tarun Gogineni, Gabriel Goh, Rapha Gontijo-Lopes, Jonathan Gordon, Morgan Grafstein, Scott Gray, Ryan Greene, Joshua Gross, Shixiang Shane Gu, Yufei Guo, Chris Hallacy, Jesse Han, Jeff Harris, Yuchen He, Mike Heaton, Johannes Heidecke, Chris Hesse, Alan Hickey, Wade Hickey, Peter Hoeschele, Brandon Houghton, Kenny Hsu, Shengli Hu, Xin Hu, Joost Huizinga, Shantanu Jain, Shawn Jain, Joanne Jang, Angela Jiang, Roger Jiang, Haozhun Jin, Denny Jin, Shino Jomoto, Billie Jonn, Heewoo Jun, Tomer Kaftan, Łukasz Kaiser, Ali Kamali, Ingmar Kanitscheider, Nitish Shirish Keskar, Tabarak Khan, Logan Kilpatrick, Jong Wook Kim, Christina Kim, Yongjik Kim, Jan Hendrik Kirchner, Jamie Kiros, Matt Knight, Daniel Kokotajlo, Łukasz Kondraciuk, Andrew Kondrich, Aris Konstantinidis, Kyle Kosic, Gretchen Krueger, Vishal Kuo, Michael Lampe, Ikai Lan, Teddy Lee, Jan Leike, Jade Leung, Daniel Levy, Chak Ming Li, Rachel Lim, Molly Lin, Stephanie Lin, Mateusz Litwin, Theresa Lopez, Ryan Lowe, Patricia Lue, Anna Makanju, Kim Malfacini, Sam Manning, Todor Markov, Yaniv Markovski, Bianca Martin, Katie Mayer, Andrew Mayne, Bob McGrew, Scott Mayer McKinney, Christine McLeavey, Paul McMillan, Jake McNeil, David Medina, Aalok

- Mehta, Jacob Menick, Luke Metz, Andrey Mishchenko, Pamela Mishkin, Vinnie Monaco, Evan Morikawa, Daniel Mossing, Tong Mu, Mira Murati, Oleg Murk, David Mély, Ashvin Nair, Reiichiro Nakano, Rajeev Nayak, Arvind Neelakantan, Richard Ngo, Hyeonwoo Noh, Long Ouyang, Cullen O’Keefe, Jakub Pachocki, Alex Paino, Joe Palermo, Ashley Pantuliano, Giambattista Parascandolo, Joel Parish, Emy Parparita, Alex Passos, Mikhail Pavlov, Andrew Peng, Adam Perelman, Filipe de Avila Belbute Peres, Michael Petrov, Henrique Ponde de Oliveira Pinto, Michael, Pokorny, Michelle Pokrass, Vitchyr H. Pong, Tolly Powell, Alethea Power, Boris Power, Elizabeth Proehl, Raul Puri, Alec Radford, Jack Rae, Aditya Ramesh, Cameron Raymond, Francis Real, Kendra Rimbach, Carl Ross, Bob Rotsted, Henri Roussez, Nick Ryder, Mario Saltarelli, Ted Sanders, Shibani Santurkar, Girish Sastry, Heather Schmidt, David Schnurr, John Schulman, Daniel Selsam, Kyla Sheppard, Toki Sherbakov, Jessica Shieh, Sarah Shoker, Pranav Shyam, Szymon Sidor, Eric Sigler, Maddie Simens, Jordan Sitkin, Katarina Slama, Ian Sohl, Benjamin Sokolowsky, Yang Song, Natalie Staudacher, Felipe Petroski Such, Natalie Summers, Ilya Sutskever, Jie Tang, Nikolas Tezak, Madeleine B. Thompson, Phil Tillet, Amin Tootoonchian, Elizabeth Tseng, Preston Tuggle, Nick Turley, Jerry Tworek, Juan Felipe Cerón Uribe, Andrea Vallone, Arun Vijayvergiya, Chelsea Voss, Carroll Wainwright, Justin Jay Wang, Alvin Wang, Ben Wang, Jonathan Ward, Jason Wei, CJ Weinmann, Akila Welihinda, Peter Welinder, Jiayi Weng, Lilian Weng, Matt Wiethoff, Dave Willner, Clemens Winter, Samuel Wolrich, Hannah Wong, Lauren Workman, Sherwin Wu, Jeff Wu, Michael Wu, Kai Xiao, Tao Xu, Sarah Yoo, Kevin Yu, Qiming Yuan, Wojciech Zaremba, Rowan Zellers, Chong Zhang, Marvin Zhang, Shengjia Zhao, Tianhao Zheng, Juntang Zhuang, William Zhuk, and Barret Zoph. Gpt-4 technical report, 2024.
- [34] Abhirama Subramanyam Penamakuri, Manish Gupta, Mithun Das Gupta, and Anand Mishra. Answer mining from a pool of images: towards retrieval-based visual question answering. *arXiv preprint arXiv:2306.16713*, 2023.
- [35] Alec Radford, Jong Wook Kim, Chris Hallacy, Aditya Ramesh, Gabriel Goh, Sandhini Agarwal, Girish Sastry, Amanda Askell, Pamela Mishkin, Jack Clark, et al. Learning transferable visual models from natural language supervision. In *International conference on machine learning*, pages 8748–8763. PMLR, 2021.
- [36] Ori Ram, Yoav Levine, Itay Dalmedigos, Dor Muhlgay, Amnon Shashua, Kevin Leyton-Brown, and Yoav Shoham. In-context retrieval-augmented language models. *Transactions of the Association for Computational Linguistics*, 11:1316–1331, 2023.
- [37] Machel Reid, Nikolay Savinov, Denis Teplyashin, Dmitry Lepikhin, Timothy Lillicrap, Jean-baptiste Alayrac, Radu Soricut, Angeliki Lazaridou, Orhan Firat, Julian Schrittwieser, et al. Gemini 1.5: Unlocking multimodal understanding across millions of tokens of context. *arXiv preprint arXiv:2403.05530*, 2024.
- [38] Weijia Shi, Sewon Min, Michihiro Yasunaga, Minjoon Seo, Rich James, Mike Lewis, Luke Zettlemoyer, and Wen-tau Yih. Replug: Retrieval-augmented black-box language models. *arXiv preprint arXiv:2301.12652*, 2023.
- [39] Amanpreet Singh, Vivek Natarajan, Meet Shah, Yu Jiang, Xinlei Chen, Dhruv Batra, Devi Parikh, and Marcus Rohrbach. Towards vqa models that can read, 2019.
- [40] Alon Talmor, Ori Yoran, Amnon Catav, Dan Lahav, Yizhong Wang, Akari Asai, Gabriel Ilharco, Hannaneh Hajishirzi, and Jonathan Berant. Multimodalqa: Complex question answering over text, tables and images. *arXiv preprint arXiv:2104.06039*, 2021.
- [41] Ryota Tanaka, Kyosuke Nishida, Kosuke Nishida, Taku Hasegawa, Itsumi Saito, and Kuniko Saito. Slidevqa: A dataset for document visual question answering on multiple images. *arXiv preprint arXiv:2301.04883*, 2023.
- [42] Google DeepMind Gemini Team. Our next-generation model: Gemini 1.5, 2024.
- [43] Rubèn Tito, Dimosthenis Karatzas, and Ernest Valveny. Document collection visual question answering. In *Document Analysis and Recognition–ICDAR 2021: 16th International Conference, Lausanne, Switzerland, September 5–10, 2021, Proceedings, Part II 16*, pages 778–792. Springer, 2021.
- [44] Angelina Wang, Alexander Liu, Ryan Zhang, Anat Kleiman, Leslie Kim, Dora Zhao, Iroha Shirai, Arvind Narayanan, and Olga Russakovsky. Revise: A tool for measuring and mitigating bias in visual datasets. *International Journal of Computer Vision*, 130(7):1790–1810, 2022.
- [45] Boxin Wang, Wei Ping, Lawrence McAfee, Peng Xu, Bo Li, Mohammad Shoeybi, and Bryan Catanzaro. Instructretro: Instruction tuning post retrieval-augmented pretraining. *arXiv preprint arXiv:2310.07713*, 2023.
- [46] Chong Xiang, Tong Wu, Zexuan Zhong, David Wagner, Danqi Chen, and Prateek Mittal. Certifiably robust rag against retrieval corruption. *arXiv preprint arXiv:2405.15556*, 2024.
- [47] Peng Xu, Wei Ping, Xianchao Wu, Lawrence McAfee, Chen Zhu, Zihan Liu, Sandeep Subramanian, Evelina Bakhurina, Mohammad Shoeybi, and Bryan Catanzaro. Retrieval meets long context large language models. *arXiv preprint arXiv:2310.03025*, 2023.
- [48] Ran Xu, Wenqi Shi, Yue Yu, Yuchen Zhuang, Yanqiao Zhu, May D Wang, Joyce C Ho, Chao Zhang, and Carl Yang. Bmretriever: Tuning large language models as better biomedical text retrievers. *arXiv preprint arXiv:2404.18443*, 2024.
- [49] Michihiro Yasunaga, Armen Aghajanyan, Weijia Shi, Rich James, Jure Leskovec, Percy Liang, Mike Lewis, Luke Zettlemoyer, and Wen-tau Yih. Retrieval-augmented multimodal language modeling. *arXiv preprint arXiv:2211.12561*, 2022.

- [50] Lijun Yu, Yong Cheng, Kihyuk Sohn, José Lezama, Han Zhang, Huiwen Chang, Alexander G Hauptmann, Ming-Hsuan Yang, Yuan Hao, Irfan Essa, et al. Magvit: Masked generative video transformer. In *Proceedings of the IEEE/CVF Conference on Computer Vision and Pattern Recognition*, pages 10459–10469, 2023.
- [51] Weihao Yu, Zhengyuan Yang, Linjie Li, Jianfeng Wang, Kevin Lin, Zicheng Liu, Xinchao Wang, and Lijuan Wang. Mm-vet: Evaluating large multimodal models for integrated capabilities, 2023.
- [52] Tianjun Zhang, Shishir G Patil, Naman Jain, Sheng Shen, Matei Zaharia, Ion Stoica, and Joseph E Gonzalez. Raft: Adapting language model to domain specific rag. *arXiv preprint arXiv:2403.10131*, 2024.

Appendix

In this appendix we discuss several additional experimental results and details not included in the main paper.

- [Appendix A](#) discusses the code release.
- [Appendix B](#) discusses the training dataset used for MIRAGE.

A Code Release

Our code and the VHS benchmark datasets are publicly available at <https://visual-haystacks.github.io>.

B MIRAGE Training Dataset

The full distribution of training data is detailed in [Figure B.1](#). In general, the data is primarily composed of multi-image augmented data from the LLaVA training set, however it also contains a mix of data from other multi-image sources including RetVQA [34], SlideVQA [41], and WebQA [7].

Number of Images/Question: 0~30

Number of Relevant Images/Question: 1~3

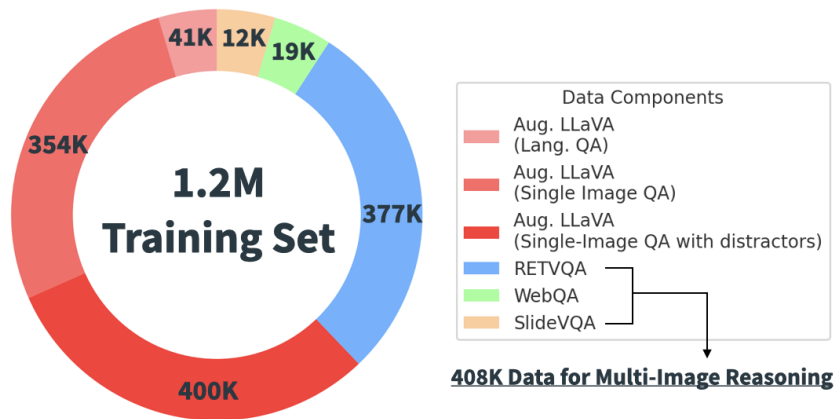


Figure B.1: Detailed Distribution of our Instruction Finetuning Data